Transition from resistive-G to η_i- driven turbulence in stellarator systems

Cite as: Physics of Fluids B: Plasma Physics 3, 1638 (1991); https://doi.org/10.1063/1.859683
Submitted: 20 March 1990 . Accepted: 28 February 1991 . Published Online: 04 June 1998

B.-G. Hong, W. Horton, S. Hamaguchi, M. Wakatani, M. Yagi, and H. Sugama

Transition from resistive-G to η_i-driven turbulence in stellarator systems

B.-G. Hong
Korea Atomic Energy Research Institute, P. O. Box 7, Dae Duk Dan Ji, Tae-Jeon, Korea
W. Horton and S. Hamaguchi
Institute for Fusion Studies, The University of Texas at Austin, Austin, Texas 78712
M. Wakatani, M. Yagi, and H. Sugama
Plasma Physics Laboratory, Kyoto University, Gokasho, Uji 611, Japan

(Received 20 March 1990; accepted 28 February 1991)

By an electromagnetic incompressible two-fluid model describing both ion temperature gradient drift modes (η_i modes) and resistive interchange modes (g modes), a new type of η_i mode is studied in cylindrical geometry including magnetic shear and an averaged curvature of Heliotron/Torsatron. This η_i mode is destabilized by the coupling to the unstable g mode. Finite plasma pressure beta increases the growth rate of this mode and the radial mode width also increases with plasma pressure beta indicating large anomalous transport in the Heliotron/Torsatron configuration. The transport from η_i mode exceeds that from resistive g when the mean-free-path exceeds the machine circumference. For plasma beta above two to three times the Suydam limit, the $m = 1/n = 1$ growth rate increases from the η_i mode value to the magnetohydrodynamic (MHD) value.

I. INTRODUCTION

Recently, electron cyclotron resonance heating (ECRH) experiments[1] in the Heliotron E showed that the ion temperature did not increase when the electron density increased at constant heating power, although the power input to the ions from the electrons was strongly enhanced. Since the electron density profile is fairly flat in the outside region and the η_i parameter is probably larger than one, the anomalous ion thermal transport driven by the η_i modes is a good candidate to explain this result. In this work, we demonstrate that the η_i modes are also destabilized by the bad average curvature, and that they couple to the g modes in the Heliotron/Torsatron. This means that the ion heat transport becomes anomalous because of the η_i mode turbulence when η_i becomes large. The difference between these two modes comes from the electron dynamics. For the η_i modes, the electrons satisfy the adiabatic (Boltzmann) relation $\tilde{n}/n_0 \simeq e\tilde{\varphi}/T_e$ in the regime of $k_\parallel^2 v_{Te}^2 > \omega\nu_{ei}$, and for the g modes, the electrons behave isothermally, $\tilde{n}/n_0 = (\omega_*/\omega)(e\tilde{\varphi}/T_e)$ in the regime of $k_\parallel^2 v_{Te}^2 < \omega\nu_{ei}$. Here, $\tilde{n}$ and $\tilde{\varphi}$ are the density and electric potential perturbations, respectively, and $k_\parallel$ is a typical parallel wave number, ω is a characteristic frequency, and ν_{ei} is the electron–ion collision frequency. Hence, the mode structure in a collisional plasma with both magnetic shear and bad average magnetic curvature will be strongly affected by the force driving the g mode in the inner region (sufficiently close to the rational surface $k_\parallel = 0$) and by the force driving the η_i mode in the outer region in the case of $\eta_i \geqslant 1$. We find that the η_i mode is further destabilized by the coupling to the resistive g mode in the sheared slab model.[2] Cordey *et al.*[3] studied a similar situation in the levitron configuration and showed that the coupling between the η_i mode and the g mode produces a single, strongly destabilized mode in the electrostatic limit.

Here, we study the coupling of the η_i mode to the resistive g mode in the cylindrical plasma with both magnetic shear and curvature of the Heliotron/Torsatron magnetic field, which is an extension of the slab model analysis showing a new type of the η_i mode.[2] Two types of eigenmodes occur in the system for the same parameters and mode numbers: One mode is radially localized and the other mode is radially global. Both the mode localized near the mode rational surface and the global mode (extending over the radius of the plasma) are studied. The global mode was not found in the slab model;[2] however, it seems similar to the nonlocal resistive drift waves obtained in the cylindrical plasma model of Heliotron E.[4] The mode with the larger growth rate is found to be the localized mode, but the global mode tends to have the larger $\gamma(\Delta r)^2$, which measures the transport. Also, we investigate the effect of finite plasma pressure beta on this new η_i mode in Heliotron/Torsatron by solving the two-coupled second-order differential eigenvalue equations for the electrostatic and parallel vector potentials.

Section II introduces the two-component dissipative hydrodynamic equations we use to derive the two-coupled second-order differential equations for the electromagnetic stability problem. Numerical solutions are given in Sec. III for a cylindrical plasma of the Heliotron E. Conclusions are given in Sec. IV.

II. MODEL EQUATIONS

We use incompressible two-fluid equations to describe the coupling of the η_i mode and the resistive g mode in the Helitron/Torsatron. The dynamical equations are derived from the two-component fluid equations using the standard reductions for low-frequency drift modes, e.g., Ref. 4. For the low m, n mode numbers considered here, the reductions use that $k_\perp\rho_i \sim \rho_i/a \ll 1$, $\nu_{ei} > \max(\omega, k_\parallel v_e)$, and $\beta = 8\pi nT/B^2 \ll 1$ so that $\delta B_\parallel/B = -4\pi\delta p/B^2$ is negligible. Both the electrostatic potential Φ and the parallel vector potential $A_\parallel$ are retained. In the parallel electron momentum equation, the electron inertia is neglected compared with the electron–ion friction since $\omega \ll \nu_{ei}$. The electron diffusion rate over the parallel wavelength $k_\parallel^2 v_e^2/\nu_{ei}$ is allowed to be either faster (η_i mode) or slower (resistive-g) than the wave frequency or growth rate. Finally, the compressibility ($\Gamma p \nabla\cdot\mathbf{v}$) is neglected in the ion thermal balance equation and the electrons are taken as isothermal ($T_e = \text{const}$) to simplify the resulting analysis. Compressibility effects, which are important in determining marginal stability, are small for the fast growing eigenmodes. Using the normalizations $e\Phi/T_e \equiv \varphi$, $n_i/n_0 \equiv n$, $\Omega_{ci}(\rho_s/a)^2 t \equiv t$, $r/a \equiv r$, and $z/R \equiv z$, we obtain the fluid model equations

$$\frac{\partial}{\partial t}\nabla_\perp^2\varphi + [\varphi,\nabla_\perp^2\varphi] + \nabla_\perp\cdot[p_i,\nabla_\perp\varphi] = -\frac{2\epsilon}{\beta_e\rho^2}\nabla_\parallel\nabla_\perp^2 A + \frac{1}{\rho^2}[p_i + n,\Omega], \tag{1}$$

$$\frac{\partial}{\partial t}v_{\parallel i} + [\varphi,v_{\parallel i}] = -\frac{\epsilon}{\rho^2}\nabla_\parallel p_i - \frac{1}{\rho^2}\frac{\partial A}{\partial t} - \frac{\epsilon}{\rho^2}\nabla_\parallel\phi + \frac{2\nu_e}{\rho^2\beta_e}\nabla_\perp^2 A, \tag{2}$$

$$\frac{\partial n}{\partial t} + [\varphi,n] = -[\varphi - n,\Omega] - \epsilon\nabla_\parallel v_{\parallel i} - \frac{2\epsilon}{\beta_e}\nabla_\parallel\nabla_\perp^2 A, \tag{3}$$

$$\frac{\partial p_i}{\partial t} + [\varphi,p_i] = 0, \tag{4}$$

$$\frac{\partial A}{\partial t} = -\epsilon(\nabla_\parallel\varphi - \nabla_\parallel n) + \frac{2\nu_e}{\beta_e}\nabla_\perp^2 A, \tag{5}$$

where $\epsilon = a/R$, $\rho = \rho_s/a$, $\beta_e = 8\pi n_0 T_e/B_0^2$, and $\nu_e = \nu_{ei}/\Omega_{ce}$. In Eqs. (1)–(5), the convective nonlinearities are written using the Poisson bracket

$$[f,g] \equiv \nabla f\times\nabla g\cdot\hat{\mathbf{z}} \quad\text{and}\quad \nabla_\parallel f \equiv \frac{\partial}{\partial z} + \frac{1}{B_0}[\Psi_0 - A,f]. \tag{6}$$

The function $\Psi_0(r)$ is the equilibrium magnetic flux function obtained from the helical magnetic fields that produce a rotational transform with the relation to a poloidal magnetic field $\mathbf{B}_p = \hat{\mathbf{z}}\times\nabla\Psi_0$. The four-field equations with different normalization in the electrostatic limit are given in Ref. 2.

A. Equilibrium

The force $\nabla\Omega(r)$ represents the averaged curvature of the magnetic field line due to the stellarator field. Since we have the average curvature without toroidicity, we employ a cylindrical geometry where all equilibrium quantities n_0, Ψ_0, and Ω depend only on r. Then the magnetic flux function Ψ_0 and the average curvature term Ω are related by

$$\Psi_0(r) = \int_0^r r'\iota(r')dr' \tag{7}$$

and

$$\Omega(r) = \frac{N\epsilon^2}{l}\left(r^2\iota(r) + 2\int_0^r r'\iota(r')dr'\right), \tag{8}$$

where $\iota(r)$ is a rotational transform, l is the poloidal number, and N is the pitch number in Stellarator/Heliotron devices.

B. Fluctuation energy density and transport

Equations (1)–(5) have an energy conservation relation in the case of $\nu_e = 0$ given by

$$\frac{\partial}{\partial t}\int dv\left(\frac{1}{2}(\nabla_\perp\phi + \nabla_\perp p_i)^2 + \frac{1}{2}v_{\parallel i}^2 + \frac{1}{2}n^2 + \frac{1}{2\beta_e}(\nabla_\perp A)^2 + np_i\right) = 0. \tag{9}$$

The nonlinear evolution of the instabilities with the invariant of Eq. (9) is for a future work. Here, we give the background evolution or balance equations obtained from Eqs. (1)–(5) after averaging over the θ-z dependence of the fluctuations. Using the notation $\bar{f} = \langle f(r,\theta,z)\rangle_{\theta,z} = f_{0,0}(r)$ and adding the background sources and sinks, the ambient or mean field equations become

$$\begin{aligned}
&\frac{\partial}{\partial t}(rv_\theta) + \frac{1}{r}\frac{\partial}{\partial r}[\Pi_\theta(r,t)] = -\frac{rj_r^{na}B}{\rho} + \frac{rF_\theta^{\text{ext}}}{\rho},\\
&\frac{\partial v_\parallel}{\partial t} + \frac{1}{r}\frac{\partial}{\partial r}(r\Pi_\parallel) = \frac{F_\parallel^{\text{ext}}}{\rho} + \mu_\parallel\nabla^2 v_\parallel,\\
&\frac{\partial N}{\partial t} + \frac{1}{r}\frac{\partial}{\partial r}(r\Gamma) = S_n,\\
&\frac{3}{2}\frac{\partial}{\partial t}P_i + \frac{1}{r}\frac{\partial}{\partial r}(rQ_i) = P_i^{\text{ext}},\\
&\frac{\partial A}{\partial t} + \frac{1}{r}\frac{\partial}{\partial r}(rF_A) = \frac{c^2\eta}{4\pi}\nabla^2 A.
\end{aligned} \tag{10}$$

The anomalous fluxes in Eqs. (10) are given by

$$\begin{aligned}
&\Pi_\theta(r,t) = r(\overline{v_\theta\delta v_{ri}}) = -\overline{\frac{\partial\varphi}{\partial r}\frac{\partial}{\partial\theta}(\varphi + \tilde{p}_i)},\\
&\Pi_\parallel(r,t) = \overline{v_\parallel\delta v_{rE}} = -\overline{\frac{v_\parallel}{r}\frac{\partial\varphi}{\partial\theta}},\\
&\Gamma(r,t) = \overline{n\delta v_{rE}} = -\overline{\frac{n}{r}\frac{\partial\varphi}{\partial\theta}},\\
&Q_i(r,t) = \frac{3}{2}\overline{p_i\delta v_{rE}} = -\frac{3}{2}\overline{\frac{p_i}{r}\frac{\partial\varphi}{\partial\theta}},\\
&F_A(r,t) = \overline{A\delta v_{re}} = -\overline{\frac{A}{r}\frac{\partial}{\partial\theta}(\varphi - \tilde{n})},
\end{aligned} \tag{11}$$

where the radial transport velocities are the ion fluid velocity v_{ri}, the electron fluid velocity v_{re} or the $\mathbf{E}\times\mathbf{B}$ velocity depending on the quantity being transported.

III. LINEAR EIGENMODES AND THEIR STABILITY

To examine the linear electromagnetic stability problem, we linearize Eqs. (1)–(5) assuming the perturbed quantities have the form of $\exp(-i\omega t + im\theta - inz)$. Following earlier work,[5] we derive the fluctuating parallel vector potential $A_\parallel$ from a new potential ψ by writing $(i\omega/c)A_\parallel = \hat{\mathbf{b}}_0\cdot\nabla\psi$ which makes

$$E_\parallel = -ik_\parallel(\phi - \psi).$$

Analysis in terms of ϕ and ψ simplifies the equations and makes the magnetohydrodynamic (MHD) polarization $\psi_{m,n}(r) \cong \phi_{m,n}(r)$ easy to recognize.

We obtain the following two-coupled second-order differential equations:

$$\left(1-\frac{\omega_{*pi}}{\omega}\right)\rho^2\nabla_r^2\phi-\left(1-\frac{\omega_{*pi}}{\omega}\right)\frac{m^2\rho^2}{r^2}\phi$$
$$=\frac{\omega_{De}-i\nu_\parallel}{\omega-\omega_{De}+i\nu_\parallel}\left\{\frac{k_\parallel^2\epsilon^2}{\omega^2\rho^2}\left(1-\frac{\omega_{*pi}}{\omega}\right)(\phi-\psi)\right.$$
$$\left.-\left(1-\frac{\omega_{*e}}{\omega}\right)\left[\phi-\left(1-\frac{\omega_{De}}{\omega}\right)\psi\right]\right\}+\frac{\omega_{De}}{\omega}$$
$$\times\left[\left(1-\frac{\omega_{*pi}}{\omega}\right)\phi-\left(1-\frac{\omega_{*e}}{\omega}\right)\psi\right], \tag{12}$$

$$-\frac{\nabla_r^2 k_\parallel\psi}{k_\parallel}+\frac{m^2}{r^2}\psi=\frac{\beta_e}{2}\frac{\omega^2}{k_\parallel^2\epsilon^2}\frac{i\nu_\parallel}{\omega-\omega_{De}+i\nu_\parallel}$$
$$\times\left\{\frac{k_\parallel^2\epsilon^2}{\omega^2\rho^2}\left(1-\frac{\omega_{*pi}}{\omega}\right)(\phi-\psi)\right.$$
$$\left.-\left(1-\frac{\omega_{*e}}{\omega}\right)\left[\phi-\left(1-\frac{\omega_{De}}{\omega}\right)\psi\right]\right\}, \tag{13}$$

where

$$\nabla_r^2=\frac{1}{r}\frac{d}{dr}r\frac{d}{dr},\quad k_\parallel(r)=m\iota(r)-n,\quad \nu_\parallel=\frac{k_\parallel^2\epsilon^2}{\nu_e},$$
$$\omega_{De}=\frac{m}{r}\frac{d\Omega}{dr}=mg,\quad \omega_{*e}=\frac{m}{r}\frac{1}{r_n},$$
$$\omega_{*pi}=-\frac{T_i}{T_e}(1+\eta_i)\omega_{*e},$$

with $\nu_e=\nu_{ei}/\omega_{ce}$. In the limit of the electrostatic approximation, Eqs. (1)–(5) reduce to Eqs. (1)–(4) of Ref. 2 in the slab limit and Eqs. (12) and (13) reduce to

$$(\omega-\omega_{*pi})\rho^2\nabla_r^2\phi-\left[(\omega-\omega_{*pi})\frac{m^2\rho^2}{r^2}-\frac{\omega_{*pi}\omega_{De}}{\omega}+i\nu_\parallel+(\omega_{De}-i\nu_\parallel)\right.$$
$$\left.\times\left(\frac{\omega_{*e}-\omega_{De}+i\nu_\parallel+(k_\parallel^2\epsilon^2/\omega\rho^2)[1-(\omega_{*pi}/\omega)]}{\omega-\omega_{De}+i\nu_\parallel}\right)\right]\phi=0. \tag{14}$$

The slab geometry version of Eq. (14) was solved in Ref. 2 and it was shown that the η_i mode is further destabilized by the coupling to the resistive-g mode. Equation (14) in the cold ion limit was studied in the cylindrical plasma by Sugama *et al.*[4] and it was found that there are two branches of the unstable modes: One localized to the mode rational surface (identified there as the resistive interchange mode) and the other is a global eigenmode, not localized to a mode rational surface (the resistive drift wave).

In the collisionless limit, with the local approximation, Eqs. (12) and (13) are analyzed for the tokamak case by Horton *et al.*[5] and it was shown that, as the plasma pressure (β) increases, the electrostatic η_i mode is strongly coupled with the finite Larmor radius (FLR)-MHD mode. In Sec. IV, the numerical solution of Eq. (14) is shown in Figs. 1–4 and the electromagnetic effect is shown in Fig. 5 by solving Eqs. (12) and (13).

IV. NUMERICAL RESULTS

Equations (12) and(13) are solved numerically for their eigenvalues and eigenfunctions using the shooting method. The parameters for the calculation are $\epsilon=a/R=0.1$, $\rho=\rho_s/a=0.02$, the background density and pressure profile $n_0 \propto p_0 \propto \exp(-2r^2)$ such that $\eta_i=1$, and the rotational transform profile of $\iota(r)=0.51+1.69r^{2.5}$, which is similar to that of Heliotron E.[6] For these parameters, the resonant surface of the $m=1/n=1$ mode, which seems to be the most dangerous mode in the Heliotron E, is at $r_0=0.61$.

We use the numerical shooting method to find the eigenmodes due to the cylindrical geometry and the two characteristic scale regions around the mode rational surface. The inner-most layer is defined by the resistive diffusion of the electrons $x_r^2=\nu_{ei}(\omega-\omega_{De})/k_\parallel'^2v_e^2$ and the outer layer by the coupling to the ion acoustic waves with $x_i^2=\omega(\omega-\omega_{*e})/k_\parallel'^2c_s^2$. Some analytic results from asymptotic matching are given in Ref. 2.

A. Electrostatic limit

Figure 1 shows the growth rate of the mode with a radial node number of $l=0,1,2$ and the global mode as a function of collision frequency $\nu_e(=\nu_{ei}/\Omega_{ce})$. Here, $g=0$ corresponds to the slab η_i mode, and $g\neq 0$ corresponds to the toroidal η_i modes within the cylindrical model. Both the global and the slab η_i modes show a weak destabilizing dependence on the collision frequency. Increasing the collision frequency enhances the growth rate of the localized mode driven by bad magnetic curvature. When the collision frequency is small, the mode with a higher radial node number ($l=2$) has a larger growth rate, but as ν_e increases, the $l=0$ mode has the largest growth rate. Also, the radial mode width of the localized $l=0$ mode increases with collision frequency because of the coupling to the resistive-g mode, indicating a stronger anomalous convective transport across the 1/1 rational surface. This tendency for the radial mode width to increase with collisionality was already found in the slab model.[2]

Figure 2 shows the dependence of the growth rate on the average curvature of the Heliotron/Torsatron. Parameters are the same as in Fig. 1 except now $\nu_e=\nu_{ei}/\omega_{ce}=5\times10^{-4}$. The growth rate of the global mode has a weak dependence on average curvature param-

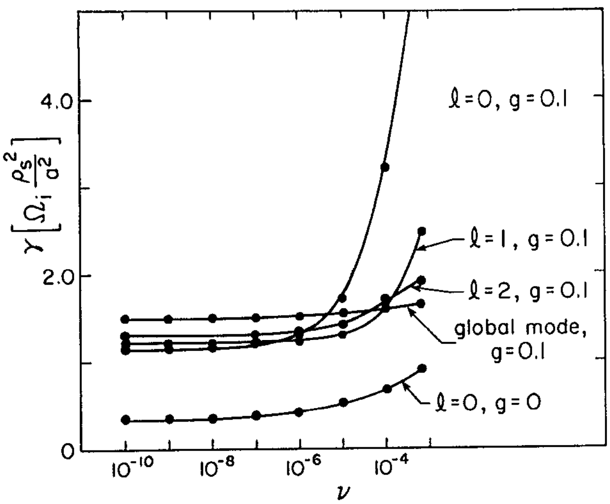

FIG. 1. Growth rate γ in units of $\Omega_{ci}(\rho_s^2/a^2)$ versus collisionality ν_{ei}/Ω_{ce}.

eter g. For the $l = 0$ localized mode, the growth rate γ increases when $g > 0$ and the effect of the negative curvature is weak.

In Fig. 3, we change the ion temperature gradient η_i parameter. In the collisionless limit [Fig. 3(a)], the threshold value is given by $\eta_c \simeq -1$, which is the usual prediction of simple incompressible, fluid theory.[7] It was shown that improved fluid theory gives $\eta_c \simeq 2/3$, which is comparable with the kinetic theory.[8] When $\nu_e = 5\times 10^{-4}$ [Fig. 3(b)], the growth rate is enhanced by a factor of 2–3, and the mode remains unstable at $\eta_i = \eta_c = -1$ because of the coupling to the resistive-g mode. Also, the $l = 0$ mode growth rate is dominant in the resistive regime.

The effect of shear on the growth rate is shown in Fig. 4. There is a stabilizing effect for the $l = 0$ mode in the collisionless and collisional case, but the effect is weak. The radial mode width depends strongly on shear with the mode

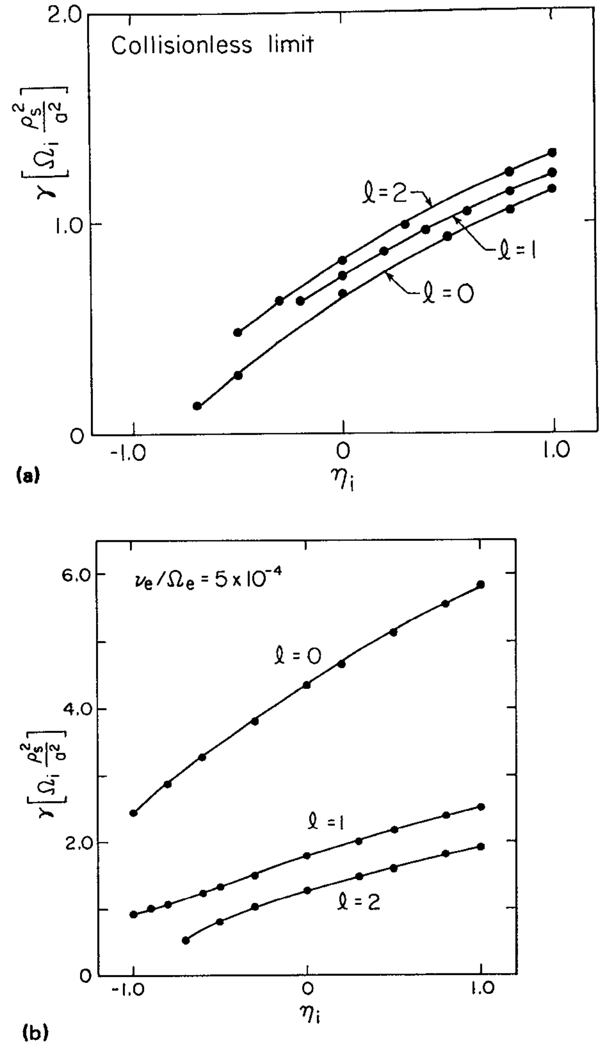

FIG. 3. Growth rate γ in units of $\Omega_{ci}(\rho_s^2/a^2)$ versus ion temperature gradient η_i for collisionless limit (a) and $\nu_{ei}/\Omega_{ce} = 5\times 10^{-4}$ (b).

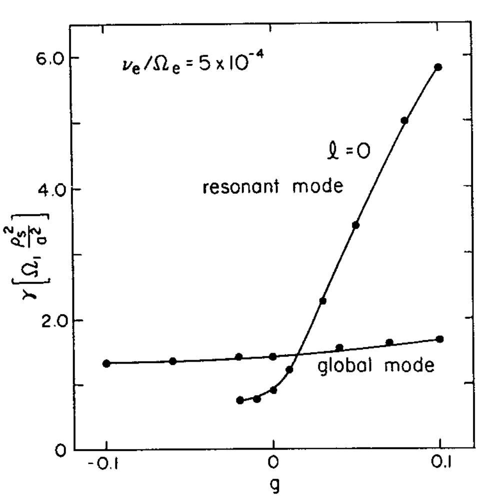

FIG. 2. Growth rate γ in units of $\Omega_{ci}(\rho_s^2/a^2)$ versus average curvature g (arbitrary unit) for $\nu_{ei}/\Omega_{ce} = 5\times 10^{-4}$.

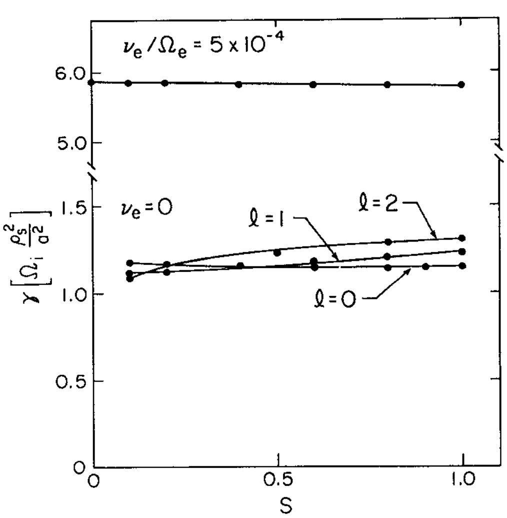

FIG. 4. Growth rate γ in units of $\Omega_{ci}(\rho_s^2/a^2)$ versus shear parameter s (arbitrary unit).

width decreasing as the shear increases, indicating a strong dependence on s of the anomalous transport. Turbulent transport theory for the resistive-g mode[9,10] and the η_i mode[5,11] gives the anomalous transport rates for $Q_i = \frac{3}{2}\overline{p_i \delta v_{rE}} \simeq -\chi_i\, dp/dr$ in Eq. (11) for resistive-g as

$$\chi_i^{r-g} = \frac{c^2\eta}{4\pi}\frac{\beta_p}{s^2}\left(\frac{r^2}{L_p R_c}\right) \simeq \nu_{ei}\rho_e^2\left(\frac{L_s^2}{L_p R_c}\right), \tag{15}$$

where β_p is the poloidal β, $s = rq'/q = qR/L_s$ is the shear parameter, L_s is the scale length of shear, R is the major radius, $q = 2\pi/\iota$ is the safety factor, and R_c is the radius of curvature and for the η_i mode in the weak shear-strong toroidicity branch,[5]

$$\chi_i^{\eta_i} \cong (\rho_s L_s / R_c^{1/2} L_{Ti}^{3/2})(cT_e/eB_p), \tag{16}$$

and for the strong shear-weak toroidicity branch[11]

$$\chi_i^{\eta_i} \cong \left(\frac{\rho_s}{L_{Ti}}\right)\left(\frac{cT_i}{eB}\right)\exp\left(\frac{-4L_{Ti}}{L_s}\right). \tag{17}$$

For all mode formulas, Eqs. (15)–(17) indicate that strong magnetic shear is the most effective mechanism for controlling the transport in both the collisional and collisionless regimes. The scaling from Eq. (15) is $\chi^{r-g} \sim nT_e^{-1/2}B_t^{-2}L_s^2L_p^{-1}R_c^{-1}$, compared with the collisionless scaling $\chi^{\eta_i} \sim T_e^{3/2}B_p^{-1}B_T^{-1}L_sR_c^{-1/2}L_p^{-3/2}$ for Eq. (16). With increasing $T_e^2/n_e \sim \lambda_{\rm mfp}/R$ the collisionless transport from Eqs. (16) and (17) quickly exceeds the collisional transport from Eq. (15).

B. High-beta electromagnetic stability

Electromagnetic effect from finite plasma pressure beta on the growth rate is shown in Fig. 5 for both the collisionless and collisional cases. As β increases, both the growth rate and the radial mode width increases, implying large $\gamma(\Delta r)^2$, which measures the anomalous transport. This destabilizing effect of the finite pressure is different from the tokamak case where the finite beta effect is related to ballooning modes; here, for the Heliotron/Torsatron, the pressure limit appears to be related to the Suydam criterion for the interchange mode in cylindrical plasma. For the same model configuration as used in Fig. 5, Sugama and Wakatani[12] find that the Suydam instability appears for $\beta(0) \geqslant \beta_{\rm crit} = 0.016$ and the growth rate becomes substantial for $\beta(0) \gtrsim 2\beta_{\rm crit} = 0.03$. It is noted that the Suydam criterion also indicates the existence of low-m mode interchange instabilities with the 1/1 mode growth rate at about 0.6γ (Suydam) when $\beta = 0.03$ according to Ref. 12.

Dominguez *et al.*[13] also show in toroidal stability theory that the Mercier criterion gives $\beta = 0.016$ for the resonant surface of $m = 1/n = 1$ using the numerical MHD toroidal equilibrium. Thus our cylindrical approximation appears good for the electromagnetic η_i mode analysis.

We find that the eigenfunction ψ increases from zero at $\beta_e = 0$ to $\psi_{1,1} \sim \frac{1}{2}\phi_{1,1}$ at $\beta_e = 0.01$ to the MHD polarization with $\psi_{1,1}(r) \simeq \phi_{1,1}(r)$ at $\beta_e = 0.02$. The eigenfunctions for the electrostatic limit and the transitional finite β_c value of $\beta_c = 0.015$ are shown in Fig. 6 for $\nu_e = 0$. As the growth rate increases with β_e, shown in Fig. 5, the wave functions broaden, approaching the MHD function at sufficiently high growth rates and β_e. A nonlocal transport may be computed from the perturbed fields ϕ, ψ, $\tilde{n}$, $v_\parallel$, and $\tilde{p}_i$ using Eqs. (10)

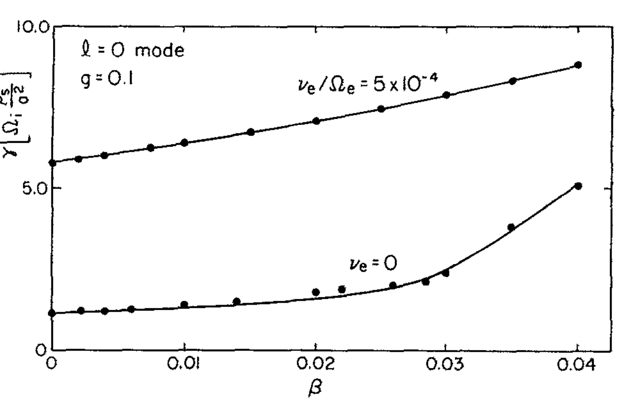

FIG. 5. Growth rate γ in units of $\Omega_{ci}(\rho_s^2/a^2)$ versus plasma pressure β for the $l = 0$ mode.

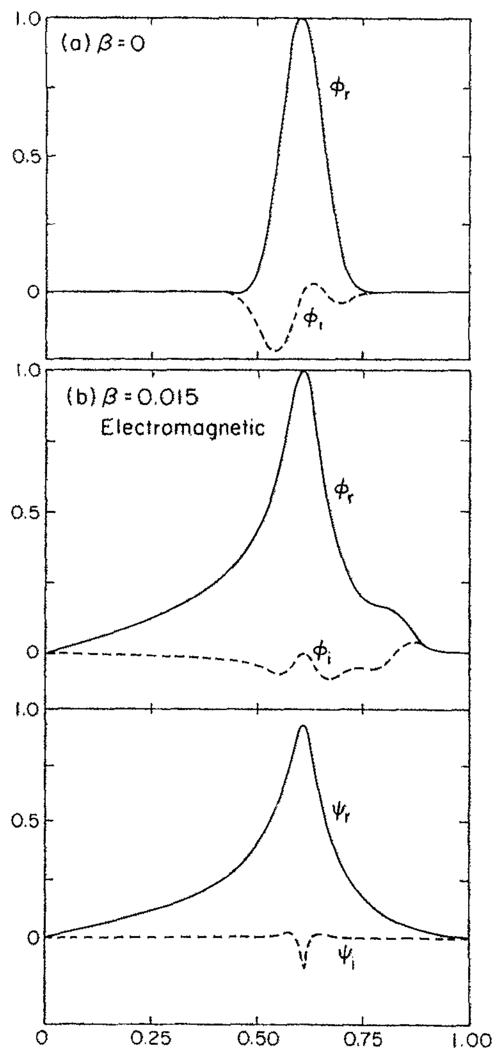

FIG. 6. Change in the eigenmode structure with increasing plasma pressure β. (a) Electrostatic mode at $\beta = 0$. (b) Electromagnetic mode at $\beta = 0.015$.

and (11). Here, we limit consideration to the local estimates given in Eqs. (15)–(17) for the localized resistive-g and η_i modes in the low-β_e limit. Finally, we find that the compressibility effect on the new η_i modes is not important, except near marginal stability for the finite g case, as demonstrated in Ref. 2. For other low-m η_i mode cases such as $m = 3/n = 2$ and $m = 5/n = 3$, no essential difference appears from the present $m = 1/n = 1$ study.

V. CONCLUSIONS

The stability analysis of the radial eigenmode equations presented here shows that there is a new type of η_i mode that is further destabilized by the coupling to the resistive-g modes in the Heliotron/Torsatron system. Both the localized and the global modes are found to be unstable in the cylindrical plasma. Including the electromagnetic component of the electromagnetic fields further enhances the growth rate of this new η_i mode implying that the instability becomes stronger with auxiliary heating in the high-density plasma. We conclude that the η_i mode is a good candidate to explain the anomalous ion thermal transport in the Heliotron E experiments. In view of these stability results, we are proceeding to the nonlinear studies of the turbulence governed by Eqs. (1)–(5).

ACKNOWLEDGMENTS

One of the authors (BGH) acknowledges Professor M. Wakatani for his support during a visit to the Plasma Physics Laboratory, Kyoto University, during the course of this work.

This work was partially supported by U. S. Department of Energy Contract No. DE-FG05-80ET-53088.

[1] H. Zushi, M. Sato, O. Motojima, S. Sudo, T. Mutoh, K. Kondo, H. Kaneko, T. Mizunehi, H. Okada, Y. Takeiri, F. Sano, A. Iiyoshi, and K. Uo, Nucl. Fusion **28**, 1801 (1988).
[2] M. Yagi, M. Wakatani, H. Sugama, B.-G. Hong, and W. Horton, J. Phys. Soc. Jpn. **12**, 4265 (1989).
[3] J. G. Cordey, E. M. Jones, and E. H. Start, Nucl. Fusion **20**, 459 (1980).
[4] H. Sugama, M. Wakatani, and A. Hasegawa, Phys. Fluids **31**, 1601 (1988).
[5] W. Horton, D.-I. Choi, and B.-G. Hong, Phys. Fluids **26**, 1461 (1983).
[6] J. H. Harris, O. Motojima, H. Kaneko, S. Besshou, H. Zushi, M. Wakatani, F. Sano, S. Sudo, A. Sasaki, K. Kondo, M. Sato, T. Mutoh, T. Mizuguchi, M. Iima, T. Obiki, A. Iiyoshi, and K. Uo, Phys. Rev. Lett. **53**, 2242 (1984).
[7] W. Horton, D.-I. Choi, and W. M. Tang, Phys. Fluids **24**, 1077 (1981).
[8] B.-G. Hong, W. Horton, and D.-I. Choi, Plasma Phys. Controlled Fusion **31**, 1291 (1989).
[9] S. Hamaguchi, Phys. Fluids B **1**, 1416 (1989).
[10] M. Yagi, M. Wakatani, and K. C. Shaing, J. Phys. Soc. Jpn. **57**, 117 (1988).
[11] S. Hamaguchi and W. Horton, Phys. Fluids B **2**, 1833 (1990).
[12] H. Sugama and M. Wakatani, J. Phys. Soc. Jpn. **58**, 1128 (1989).
[13] N. Dominguez, J.-N. Leboeuf, B. A. Carreras, and V. E. Lynch, Nucl. Fusion **29**, 2079 (1989).